ORGANIC LETTERS

2013
Vol. 15, No. 21
5488–5491

Lingzhiols, Unprecedented Rotary Door-Shaped Meroterpenoids as Potent and Selective Inhibitors of p-Smad3 from *Ganoderma lucidum*

Yong-Ming Yan,[†,‡,⊥] Jun Ai,[§,⊥] Li−Li Zhou,[§,⊥] Arthur C.K. Chung,[∥,⊥] Rong Li,[∥] Jing Nie,[§] Ping Fang,[†] Xin-Long Wang,[†] Jie Luo,[†] Qun Hu,[†] Fan-Fan Hou,[*,§] and Yong-Xian Cheng[*,†]

State Key Laboratory of Phytochemistry and Plant Resources in West China, Kunming Institute of Botany, Chinese Academy of Sciences, 132 Lanhei Road, Kunming 650201, P. R. China, Division of Nephrology, Nanfang Hospital, Southern Medical University, Key Laboratory for Organ Failure Research, Education Ministry, Guangzhou 510515, P. R. China, University of Chinese Academy of Sciences, Yuquan Road 19, Beijing 100049, P. R. China, and Department of Medicine and Therapeutics, Li Ka Shing Institute of Health Sciences, The Chinese University of Hong Kong, Shatin, New Territories, Hong Kong SAR, P. R. China

yxcheng@mail.kib.ac.cn; ffhouguangzhou@163.com

Received September 12, 2013

ABSTRACT

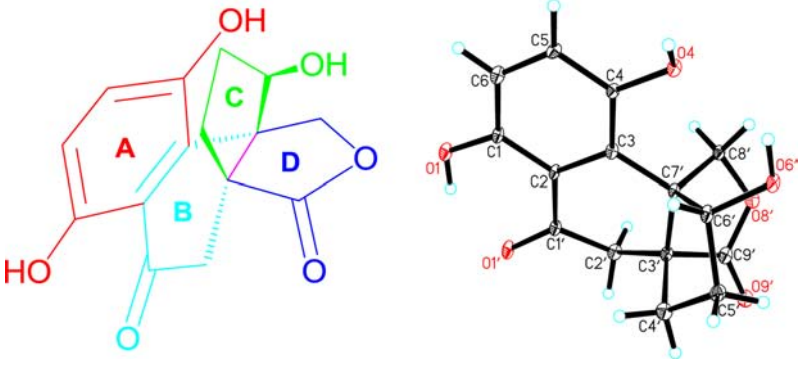

(+)-Lingzhiol and (−)-lingzhiol, a pair of rotary door-shaped meroterpenoidal enantiomers, were isolated from *Ganoderma lucidum*. Their structures were identified by spectroscopic methods and X-ray diffraction crystallography. Lingzhiol bears an unusual 5/5/6/6 ring system characteristic of sharing a C-3′−C-7′ axis. Biological evaluation showed that (+)-lingzhiol or (−)-lingzhiol could selectively inhibit the phosphorylation of Smad3 in TGF-β1-induced rat renal proximal tubular cells and activate Nrf2/Keap1 in mesangial cells under diabetic conditions.

Diabetic nephropathy (DN), as a major complication of diabetes, is increasing rapidly around the world. Because of the limited availability of efficacious drugs, DN has become a major threat for diabetes mellitus patients.[1] Renal fibrosis is a hallmark of chronic kidney disease; many pathogenic processes are involved in renal fibrosis such as growth factors, cytokines, and stress molecules. Although great efforts have been made in recent years, efficient treatment for DN and renal fibrosis still remains unresolved. Studies show that multiple pathogenic factors such as oxidative stress, chronic inflammation, accumulation of extracellular matrix (ECM), and TGF-β/Smads signaling pathways are involved in DN and renal

[†] Kunming Institute of Botany, Chinese Academy of Sciences.
[‡] University of Chinese Academy of Sciences.
[§] Southern Medical University.
[∥] The Chinese University of Hong Kong.
[⊥] These authors contributed equally to this paper.

(1) Navarro-González, J. F.; Mora-Fernández, C. *J. Am. Soc. Nephrol.* **2008**, *19*, 433–442.
(2) Ha, H.; Hwang, I. A.; Park, J. H.; Lee, H. B. *Diabetes Res. Clin. Pract.* **2008**, *82s*, s42–s45.
(3) Ziyadeh, F. N. *Am. J. Kidney Dis.* **1993**, *22*, 736–744.

10.1021/ol4026364
Published on Web 10/15/2013

fibrosis,[2−4] and therefore, have become targets for DN and renal fibrosis drug discovery.

The search for drug leads against chronic kidney disease including DN and renal fibrosis has become our research focus in recent years. *Ganoderma lucidum*, commonly known as Lingzhi in China, belonging to the genus *Ganoderma*, which includes about 80 species, is a well-known mushroom in the Orient because of its extensive uses in traditional Asian medicines; it has now also gained recognition in the West. Various medicinal properties of *G. lucidum* have attracted great interest in the past. To date, hundreds of compounds have been identified from this genus; many of them are triterpenoids and polysaccharides.[5] We hypothesized that *G. lucidum* may contain antichronic kidney disease compounds as indicated by its clinical applications.[6] We thus began an investigation on this species, which led to the isolation of compound **1** with a novel 5/5/6/6 ring system: three rings in **1** sharing a C-3′−C-7′ axis made the structure rotary doorlike.

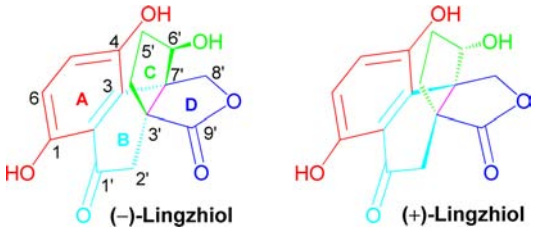

Lingzhiol (**1**)[7] was obtained as a yellowish crystal (cyclohexane/Me_2CO, 1:1). Its molecular formula, $C_{15}H_{14}O_6$, was determined by means of HREIMS (*m*/*z* 290.0794 $[M]^+$, calcd for 290.0790), ^{13}C, and DEPT NMR spectra, having 9 degrees of unsaturation. The ^1H NMR spectrum (Table 1) demonstrated two doublets (δ_H 7.22, d, J = 8.9 Hz, H-5; δ_H 6.77, d, J = 8.9 Hz, H-6) in the olefinic region, corresponding to an AB aromatic system, two $^2J_{H,H}$ coupling protons (δ_H 3.09, d, J = 16.0 Hz, Ha-2′; δ_H 2.79, d, J = 16.0 Hz, Hb-2′), one oxygenated methylene (δ_H 5.22, d, J = 9.6 Hz, Ha-8′; δ_H 4.45, d, J = 9.6 Hz, Hb-8′), and one oxygenated methine (δ_H 4.63, t-like, J = 4.5 Hz, H-6′). In addition, two methylenes behaving as multiplicities upfield were also observed in the ^1H NMR spectrum. The ^{13}C and DEPT NMR spectra (Table 1) gave 15 carbons, which were classified as four methylenes (one oxygenated), three methines (two olefinic, one oxygenated), and eight quaternary carbons (one ketone, one ester carbonyl, four olefinic including two oxygenated, and two aliphatic). The NMR data of **1** partly resembled those of fornicin A previously isolated from *G. fornicatum*,[8] implying that they are analogues, either from a chemical or from a biogenic point of view. The difference at the benzene ring was that an ABX coupling system in fornicin A was replaced by an AB coupling pattern in **1**, indicating a 1,2,3,4-tetrasubstituted benzene ring in **1**. The $^1H-^1H$ COSY spectrum showed correlations of H-5/H-6, H-4′/H-5′/H-6′ (Figure 1). The construction of **1** was mainly performed by extensive HMBC experiment (Figure 1), which showed correlations of H-6/C-1 (δ_C 156.3), C-2 (δ_C 116.4), H-2′/C-1′ (δ_C 202.3), and C-2 suggesting the presence of a benzoyl group, in accordance with UV absorptions at 374 and 266 nm. The HMBC correlations of H-4′/C-2′, C-3′, and C-9′ (δ_C 180.1) and H-2′/C-3′, C-4′, and C-9′ indicated that a methylene and a methyl of one isoprenyl group were both oxidized to a ketone and a carboxylic carbonyl, respectively. The structure fragment was further extended by the HMBC correlations of H-6′/C-7′, and C-3; this clearly indicated that C-6′ was connected to C-3 via C-7′. We noted that C-3′ and C-7′ were both aliphatic quaternary carbons. H-2′ and H-4′ both correlating with C-7′, H-6′/C-8′ (δ_C 70.9), H-8′/C-6′, C-7′, C-3′, and C-3 suggested the linkage of C-3′−C-7′ and C-7′−C-8′ and confirmed the connection of C-3−C-7′. So far, rings A, B, and D have been formed. Apart from three rings including a benzene ring, two carbonyls accounting for 8 degrees of unsaturation, an additional ring is required to form structure **1**. The HMBC correlation of H-8′/C-9′ with consideration of chemical shifts of H-8′ or C-8′ indicated the presence of a five-membered lactone, agreeing with the IR absorption at 1757 cm^{-1}. The formation of ring C allowed structure **1** to possess three rings sharing a common C3′−C7′ axis.

Table 1. ^1H (400 MHz) and ^{13}C NMR (100 MHz) Data of **1** in Acetone-d_6 (δ, ppm)

	compound **1**	
position	δ_C, mult	δ_H, (mult, J in Hz)
1	156.3 s	
2	116.4 s	
3	129.1 s	
4	147.9 s	
5	127.5 d	7.22 (d, 8.9)
6	117.9 d	6.77 (d, 8.9)
1′	202.3 s	
2′a	42.3 t	3.09 (d, 16.0)
2′b		2.79 (d, 16.0)
3′	52.5 s	
4′a	33.3 t	2.44 m
4′b		1.78 m
5′a	33.7 t	1.83 m
5′b		1.70 m
6′	80.6 d	4.63 (t-like, 4.5)
7′	56.1 s	
8′a	70.9 t	5.22 (d, 9.6)
8′b		4.45 (d, 9.6)
9′	180.1 s	

The existence of rings B−D brought a natural rigidity to the molecule. This meant that C-8′ and C-9′ should be at the same face of rings B and D. This assumption was

(4) Brownlee, M. *Nature* **2001**, *414*, 813–820.
(5) Shiao, M. S. *Chem. Rec.* **2003**, *3*, 172–180.
(6) Qu, L.; Wang, X. S.; Cao, A. G. *Gansu J. TCM* **2011**, *24*, 28–29.
(7) Lingzhiol (**1**): yellowish crystals; UV λ_{max} (MeOH) (log ε) 374 (3.59), 266 (3.73), 235 (3.91) nm; IR (KBr) ν_{max} 3536, 3441, 3426, 3237, 1757, 1653, 1591, 1475, 1458, 1328, 1313, 1291, 1208, 1130, 1100, 1011 cm^{-1}; ^1H and ^{13}C NMR spectroscopic data, see Table 1; ESIMS (negative) *m*/*z* 289 $[M - H]^-$; HREIMS *m*/*z* 290.0794 $[M]^+$ (calcd for $C_{15}H_{14}O_6$, 290.0790). $[[\alpha]^{19}_D$ +90.5 (*c* 0.36, MeOH); CD (MeOH) $\Delta\varepsilon_{214}$ −24.56, $\Delta\varepsilon_{241}$ 5.14, $\Delta\varepsilon_{265}$ 9.91, $\Delta\varepsilon_{314}$ 3.66, $\Delta\varepsilon_{373}$ −2.04; (+)-lingzhiol]; $[[\alpha]^{19}_D$ −94.2 (*c* 0.36, MeOH); CD (MeOH) $\Delta\varepsilon_{214}$ 26.85, $\Delta\varepsilon_{241}$ − 6.46, $\Delta\varepsilon_{265}$ − 11.20, $\Delta\varepsilon_{314}$ − 3.89, $\Delta\varepsilon_{373}$ 1.88; (−)-lingzhiol].
(8) Niu, X. M.; Li, S. H.; Sun, H. D.; Che, C. T. *J. Nat. Prod.* **2006**, *69*, 1364–1369.

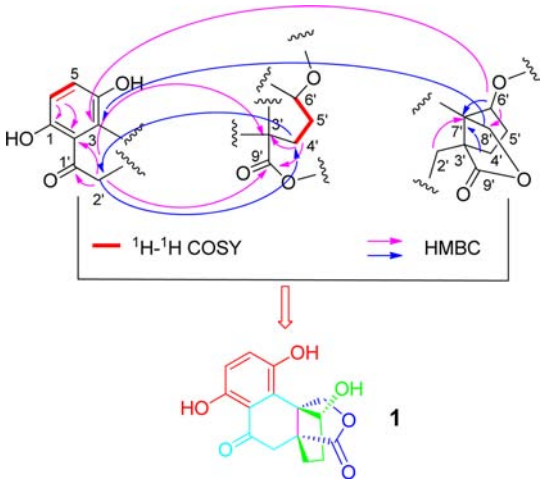

Figure 1. Key ^{1}H−^{1}H COSY and HMBC correlations for (±)-**1**.

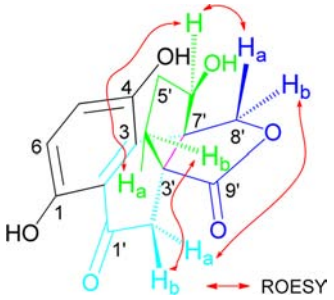

Figure 2. Important ROESY correlations of (±)-**1**.

confirmed by the observed ROESY correlations (Figure 2) of H-6′/Ha-4′. The ROESY cross peaks of Ha-2′/Hb-8′, and H-6′/Ha-8′ suggested that these protons are spatially vicinal. Although the ROESY correlations of Hb-2′/Hb-4′, H-6′/Ha-4′, and Ha-8′ were observed, it was not useful to assign the configuration at C-6′. The orientation of a hydroxyl group at C-6′ was finally determined as shown by single crystal X-ray diffraction.[9] The optical rotation value and the space group *Pna*21 of **1** indicated a racemic nature, which was subsequently purified by HPLC column on a chiral phase to afford two enantiomers, (+)-**1** and (−)-**1**, showing opposite Cotton effects at the range of 195−420 nm in the CD spectra (Figure S11). Finally, single-crystal (cyclohexane/EtOH, 3:2) X-ray diffraction analyses of (−)-**1** assigned its absolute configuration as 3′*R*,6′*R*,7′*R* (Figure 3).

Meroterpenoids are defined as natural products produced from polyketide and terpenoid precursors.

(9) Crystallographic data of lingzhiol (**1**) have been deposited at the Cambridge Crystallographic Data Centre (deposition no. CCDC 959365 for (±)-**1**, CCDC 963800 for (−)-**1**). Copies of these data can be obtained free of charge via www.ccdc.cam.ac.uk/conts/retrieving.html.

Figure 3. X-ray crystallographic structure of (−)-**1**.

Compound **1** is a meroterpenoid formed by a substituted benzene ring and a terpenoid. Compared to fornicin A, a "tail" carbon of one isoprenyl moiety was missing in the structure of **1**, which actually made **1** a normeroterpenoid. A plausible biosynthetic pathway of **1** is proposed as shown in Scheme 1 (Supporting Information). Meroterpenoids have been characterized from the *Ganoderma* species,[8,10] however, this is the first time that we isolated a meroterpenoid bearing a 5/5/6/6 ring system.

In consideration of traditional Chinese medicinal uses of *G. lucidum*, and with the motivation to search for leads against chronic kidney disease, compounds (+)-**1** and (−)-**1** were purposely tested for their inhibitory effects on reactive oxygen species (ROS), collagen IV (Col IV), fibronectin (FN), and IL-6 production in high-glucose-induced mesangial cells using previously described methods.[11,12] The results showed that both (+)-**1** and (−)-**1** could significantly inhibit high-glucose-induced ROS (Figure S12), collagen IV, fibronectin, and IL-6 (Figure 4) generation in a dose-dependent manner. In addition, we found no significant difference among the groups in a cytotoxicity assay used to exclude possible cellular toxicity effects.

Indeed, ROS play an essential role in chronic kidney diseases, and high-glucose-induced overproduction of ROS is the key initiator in the pathogenesis of DN,[4] which damage cells directly and indirectly.[13,14] Indeed, inhibition of ROS production is demonstrated to be effective in retarding the progress of DN.[15] As shown in Figure S12,

(10) Adams, M.; Christen, M.; Plitzko, I.; Zimmermann, S.; Brun, R.; Kaiser, M.; Hamburger, M. *J. Nat. Prod.* **2010**, *73*, 897–900.

(11) (a) Xia, L.; Wang, H.; Goldberg, H. J.; Munk, S.; Fantus, I. G.; Whiteside, C. I. *Am. J. Physiol. Renal Physiol.* **2006**, *290*, F345–F356. (b) Xia, L.; Wang, H.; Muunk, S.; Frecker, H.; Goldberg, H. J.; Fantus, I. G.; Whiteside, C. I. *Am. J. Physiol. Endocrinol. Metab.* **2007**, *293*, E1280–E1288. (c) Ha, H.; Yu, M. R.; Choi, Y. J.; Kitamura, M.; Lee, H. B. *J. Am. Soc. Nephrol.* **2002**, *13*, 894–902.

(12) Min, D. Q.; Lyons, J. G.; Bonner, J.; Twigg, S. M.; Yue, D. K.; McLennan, S. V. *Am. J. Physiol. Renal Physiol.* **2009**, *297*, F1229–F1237.

(13) Lee, E. A.; Seo, J. Y.; Jiang, Z.; Yu, M. R.; Kwon, M. K.; Ha, H.; Lee, H. B. *Kidney Int.* **2005**, *67*, 1762–1771.

(14) Lee, H. B.; Yu, M. R.; Yang, Y.; Jiang, Z. *J. Am. Soc. Nephrol.* **2003**, *14*, S241–S245.

(15) Romeo, L.; Intrieri, M.; D'Agata, V.; Mangano, N. G.; Oriani, G.; Ontario, M. L.; Scapagnini, G. *J. Am. Coll. Nutr.* **2009**, *28*, 492S–499S.

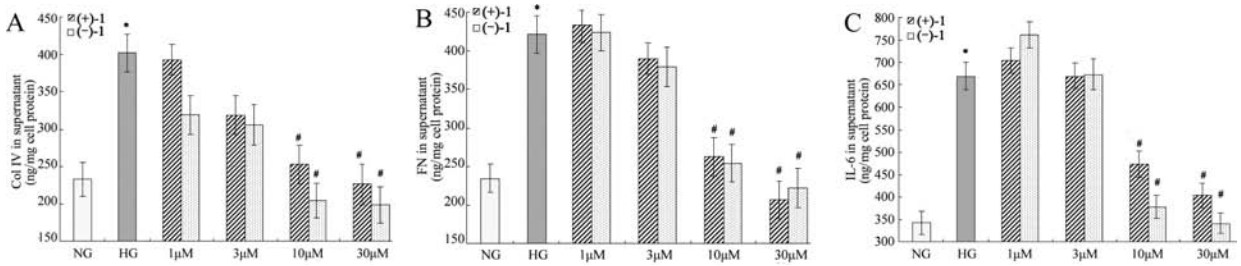

Figure 4. Compound (−)-**1** or (+)-**1** inhibited collagen IV (Col IV) (A), fibronectin (FN) (B), and IL-6 (C) over production in a dose-dependent manner. $^{*}p < 0.05$ vs NG; $^{\#}p < 0.05$ vs HG.

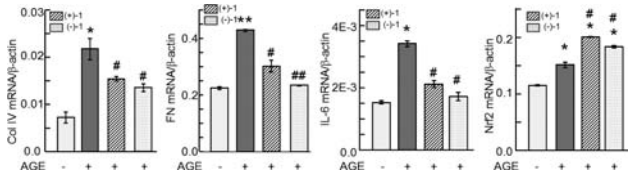

Figure 5. Compound (−)-**1** or (+)-**1** inhibited transcript levels of collagen IV (Col IV), fibronectin (FN), and IL-6 but induced Nrf2 in mesangial cells under diabetic conditions at 10 μM. $^{*}p < 0.05$, $^{**}p < 0.01$ vs no AGE; $^{\#}p < 0.05$, $^{\#\#}p < 0.01$ vs AGE alone. AGE: advanced glycation end product.

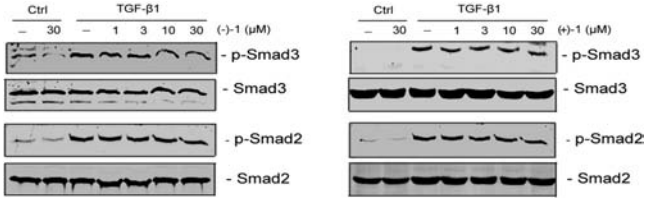

Figure 6. Compound (−)-**1** or (+)-**1** selectively blocked TGF-β1-mediated Smad3 phosphorylation in a dose-dependent manner. NRK-52E cells were treated with TGF-β1 (10 ng/mL) for 1 h in the absence or presence of different doses of (+)-**1** or (−)-**1** as indicated.

(−)-**1** potently inhibits ROS production and is a promissing inhibitor of ROS generation.

It is known that ROS over production will evoke cell defense to combat ROS and oxidative damage. Cellular defense toward ROS occurs by an antioxidant responsive element.[16] Among these, nuclear factor erythroid 2-related factor 2 (Nrf2) is a transcription factor specifically activated by oxidative and electrophilic stimulation, which up-regulates the expression of antioxidant genes to pretect cells from damage.[17] We thus checked whether (+)-**1** and (−)-**1** could activate Nrf2 by quantitative realtime-PCR analyses. The results showed that either (+)-**1** or (−)-**1** further induced Nrf2 transcript levels and suppressed collagan IV, FN, and IL-6 in mesangial cells under diabetic conditions (Figure 5).

Chronic inflammation and ECM accumulation is seen in the pathogenisis of DN and renal fibrosis. It is known that the TGF-β/Smads pathway plays an important role in these diseases among multiple mechanisms. Normally, the phosphorylation of Smad3 and Smad2 is simultaneously activated in the context of kidney diseases.[18] Our study showed that the phosphorylation of Smad3 but not of Smad2 could be significantly inhibited by (−)-**1** in TGF-β1-induced rat renal proximal tubular cells (NRK-52E) (Figure 6 and Figure S13, Supporting Information) and to a lesser extent by (+)-**1**, indicating that these compounds are selective inhibitors of p-Smad3. To our knowledge, small molecule p-Smad3 inhibitors are very rare to date; these enantiomers represent the leading example of natural selective p-Smad3 inhibitors. A recent study showed that Smad2 activation plays a renoprotective role in kidney fibrosis[19] and the activation of p-Smad2 was not affected by (+)-**1** and (−)-**1**, indicating that they have dual protective role in kidney diseases. Further mechanistic studies of (−)-**1** and its in vivo effects are underway in our group.

Acknowledgment. This work was supported financially by the NSFC-Joint Foundation of Yunnan Province (U1202222), a project from State Key Laboratory of Phytochemistry and Plant Resources in West China, Kunming Institute of Botany (P2013-ZZ03), and Research Grant Council of Hong Kong (GRF 463612 to ACK Chung).

Supporting Information Available. 1D, 2D NMR, MS, IR, and CD spectra, detailed isolation procedures, bioassay methods, partial biological data, a plausible biosynthetic pathway of **1**, and X-ray crystal data of (±)-**1** and (−)-**1**. This material is available free of charge via Internet at http://pubs.acs.org.

(16) Friling, R. S.; Bensimon, A.; Tichauer, Y.; Daniel, V. *Proc. Natl. Acad. Sci. U.S.A.* **1990**, *87*, 6258–6262.
(17) Itoh, K.; Tong, K. I.; Yamamoto, M. *Free Radic. Biol. Med.* **2004**, *36*, 1208–1213.
(18) Lan, H. Y. *Kidney Res. Clin. Pract.* **2012**, *31*, 4–11.
(19) Meng, X. M.; Huang, X. R; Chung, A. C.; Qin, W.; Shao, X.; Igarashi, P.; Ju, W.; Bottinger, E. P.; Lan, H. Y. *J. Am. Soc. Nephrol.* **2010**, *21*, 1477–1487.

The authors declare no competing financial interest.